

Molecular Dynamics of Thermotropic Liquid Crystals: Anomalous relaxation dynamics of calamitic and discotic liquid crystals

Biman Jana AND Biman Bagchi

Abstract | Recent optical kerr effect (OKE) studies have demonstrated that orientational relaxation of rod-like nematogens exhibits temporal power law decay at intermediate times not only near the isotropic–nematic (I–N) phase boundary but also in the nematic phase. Such behaviour has drawn an intriguing analogy with supercooled liquids. We have investigated both collective and single-particle orientational dynamics of a family of model system of thermotropic liquid crystals using extensive computer simulations. Several remarkable features of glassy dynamics are on display including non-exponential relaxation, dynamical heterogeneity, and non-Arrhenius temperature dependence of the orientational relaxation time. Over a temperature range near the I–N phase boundary, the system behaves remarkably like a fragile glass-forming liquid. Using proper scaling, we construct the usual relaxation time versus inverse temperature plot and explicitly demonstrate that one can successfully define a density dependent fragility of liquid crystals. The fragility of liquid crystals shows a temperature and density dependence which is remarkably similar to the fragility of glass forming supercooled liquids. Energy landscape analysis of inherent structures shows that the breakdown of the Arrhenius temperature dependence of relaxation rate occurs at a temperature that marks the onset of the growth of the depth of the potential energy minima explored by the system. A model liquid crystal, consisting of disk-like molecules, has also been investigated in molecular dynamics simulations for orientational relaxation along two isobars starting from the high temperature isotropic phase. The isobars have been so chosen that the phase sequence isotropic (I)–nematic (N)–columnar (C) appears upon cooling along one of them and the sequence isotropic (I)–columnar (C) along the other. While the orientational relaxation in the isotropic phase near the I–N phase transition shows a power law decay at short to intermediate times, such power law relaxation is not observed in the isotropic phase near the I–C phase boundary. The origin of the power law decay in the single-particle second-rank orientational time correlation function (OTCF) is traced to the growth of the orientational pair distribution functions near the I–N phase boundary. As the system settles into the nematic phase, the decay of the single-particle second-rank orientational OTCF follows a pattern that is similar to what is observed with calamitic liquid crystals and supercooled molecular liquids.

*Solid State and Structural
Chemistry Unit, Indian
Institute of Science,
Bangalore 560012, India
bbagchi@sscu.iisc.ernet.in*

Introduction

Thermotropic liquid crystals exhibit exotic phase behavior upon temperature variation. In the isotropic phase, a liquid does not exhibit any long

range translational or orientational order. The nematic phase is endowed with a long-ranged orientational order but lacks translational order. Further cooling leads to a more ordered smectic

phase where two-dimensional translational order along with long-ranged orientational order sets in the system. The isotropic-nematic (I–N) phase transition, which is believed to be weakly first order in nature with certain characteristics of the continuous transition, has been a subject of immense attention in condensed matter physics and material sciences.^{1,2} In contrast, the dynamics of thermotropic liquid crystals have been much less studied, the focus being mostly on the long-time behavior of orientational relaxation near the I–N transition.¹ A series of OKE measurements have, however, recently studied collective orientational relaxation in the isotropic phase near the I–N transition over a wide range of time scales.^{3,4} The dynamics have been found to be surprisingly rich, the most intriguing feature being the power law decay of the OKE signal at short-to-intermediate times.^{3,4} The relaxation scenario appears to be strikingly similar to that of supercooled molecular liquids⁵, even though the latter do not undergo any thermodynamic phase transition.

This work essentially consists of two parts. In the first part we study dynamics of rod-like molecules that form calamitic liquid crystal. In the second part, we study the dynamics of disk-like molecules that form discotic phase. Despite such a large difference in aspect ratio and nature of the nematic liquid crystals that they form, there are aspects of relaxation that are remarkably similar. However, a molecular level understanding of observed anomalous orientational dynamics is missing.

Relaxation of discotic phases has been less explored than that of calamitic liquid crystals. The discovery of discotic liquid crystals, that consist of disk-like molecules is more recent and dates back only to the late 1970⁶. Upon cooling from the high temperature isotropic (I) phase, discotic liquid crystals typically exhibit a nematic (N) phase and/or a columnar (C) phase⁷. The discotic nematic phase is analogous to the nematic phase formed by rodlike molecules in that there is a long-range orientational order without the involvement of any long-range translational order. In the columnar phase that is typical of discotic liquid crystals, the molecules are stacked on top of each other giving rise to a columnar structure. These columns form a long-range two dimensional order in the orthogonal plane with either a hexagonal or a rectangular symmetry. While the sequence of phases I–N–C has been observed experimentally with a number of discotic liquid crystals upon cooling, there have been only a few cases where only I–C or I–N transition is observed⁸. Although computer simulations of model liquid crystals have undergone an upsurge

in recent times, discotic liquid crystals are yet to be studied in detail. Discotic molecules typically contain an aromatic core with flexible chains added in the equatorial plane. While atomistic models could in principle be undertaken, molecular models, where mesogens are approximated with particles with well-defined anisotropic shape, find their utility in obtaining a rather generalized view. A simple approach along this line involves consideration of purely repulsive models involving hard bodies⁹. This rather extreme choice is inspired by the idea that the equilibrium structure of a dense liquid is essentially determined by the repulsive forces which fix the molecular shape. Along this line, thin hard platelets, hard oblate ellipsoids of revolution, and cut hard spheres have been investigated. Such an approach is appealing for its simplicity⁹. However, temperature plays no direct role in purely repulsive models on the contrary to what is desired for thermotropic liquid crystals⁹. In this respect, the Gay-Berne pair potential¹⁰, which is essentially a generalization of the Lennard-Jones potential to incorporate anisotropic interactions, or one of its variants¹⁰, where mesogens are approximated with soft ellipsoids of revolution, appears to serve as a more realistic model. In fact, discotic liquid crystals, modeled by the Gay-Berne family of potentials, have been found to capture the key features of the experimentally observed phase behavior¹¹.

In this article, we present results of molecular dynamics simulations of a family of model systems consisting of both rod-like and disk-like molecules across the I–N and I–C transition. Given the involvement of the phase transition to an orientationally ordered mesophase upon lowering the temperature, we choose to probe the single-particle and collective orientational dynamics in order to make comparison with relaxation behaviour observed for supercooled liquids. We have calculated the non-Gaussian parameter in the orientational degrees of freedom in order to probe the heterogeneous dynamics present in the system near I–N transition. We have defined a fragility index to quantitatively measure the glassy dynamics observed in the orientational degrees of freedom. We have also explored plausible correlation of the features of the underlying energy landscape with the observed non-Arrhenius dynamics in analogy with supercooled liquids. This work follows up our recent work¹², which has reported the emergence of power law decay regime(s) in orientational relaxation across the isotropic-nematic transition. In the spirit of the universal power law in orientational relaxation in thermotropic liquid crystals suggested therein¹², we compare the orientational dynamics we observed here with those of calamitic liquid crystals obtained from recent optical Kerr effect measurements and molecular dynamics simulations studies. We further discuss the analogous dynamics observed in supercooled molecular liquids.

Models and simulation details

A. Rod-like molecules

The systems we have studied consist of ellipsoids of revolution. The Gay-Berne (GB) pair potential¹⁰, that is well established to serve as a model potential for systems of thermotropic liquid crystals, has been employed. The GB pair potential, which uses a single-site representation for each ellipsoid of revolution, is an elegant generalization of the extensively used isotropic Lennard-Jones potential to incorporate anisotropy in both the attractive and the repulsive parts of the interaction^{10,11}. In the GB pair potential, i th ellipsoid of revolution is represented by the position \mathbf{r}_i of its center of mass and a unit vector \mathbf{e}_i along the long axis of the ellipsoid. The interaction potential between two ellipsoids of revolution i and j is given by

$$U_{ij}^{GB} = 4\varepsilon(\hat{\mathbf{r}}_{ij}, \mathbf{e}_i, \mathbf{e}_j) \left(\rho_{ij}^{-12} - \rho_{ij}^{-6} \right) \quad (1)$$

where

$$\rho_{ij} = \frac{r_{ij} - \sigma(\hat{\mathbf{r}}_{ij}, \mathbf{e}_i, \mathbf{e}_j) + \sigma_{ss}}{\sigma_{ss}} \quad (2)$$

Here σ_{ss} defines the thickness or equivalently, the separation between the two ellipsoids of revolution in a side-by-side configuration, r_{ij} is the distance between the centers of mass of the ellipsoids of revolution i and j , and $\hat{\mathbf{r}}_{ij} = \mathbf{r}_{ij}/r_{ij}$ is a unit vector along the intermolecular separation vector \mathbf{r}_{ij} . The molecular shape parameter σ and the energy parameter ε both depend on the unit vectors \mathbf{e}_i and \mathbf{e}_j as well as on $\hat{\mathbf{r}}_{ij}$ as given by the following set of equations:

$$\sigma_{ij}(\hat{\mathbf{r}}_{ij}, \mathbf{e}_i, \mathbf{e}_j) = \sigma_0 \left[1 - \frac{\chi}{2} \left\{ \frac{(\mathbf{e}_i \cdot \hat{\mathbf{r}}_{ij} + \mathbf{e}_j \cdot \hat{\mathbf{r}}_{ij})^2}{1 + \chi(\mathbf{e}_i \cdot \mathbf{e}_j)} - \frac{(\mathbf{e}_i \cdot \hat{\mathbf{r}}_{ij} - \mathbf{e}_j \cdot \hat{\mathbf{r}}_{ij})^2}{1 - \chi(\mathbf{e}_i \cdot \mathbf{e}_j)} \right\} \right]^{-1/2} \quad (3)$$

with $\chi = (\kappa^2 + 1)/(\kappa^2 - 1)$ and

$$\varepsilon(\hat{\mathbf{r}}_{ij}, \mathbf{e}_i, \mathbf{e}_j) = \varepsilon_0 [\varepsilon_1(\mathbf{e}_i, \mathbf{e}_j)]^\nu [\varepsilon_2(\hat{\mathbf{r}}_{ij}, \mathbf{e}_i, \mathbf{e}_j)]^\mu \quad (4)$$

where the exponents ν and μ are the adjustable parameter, and

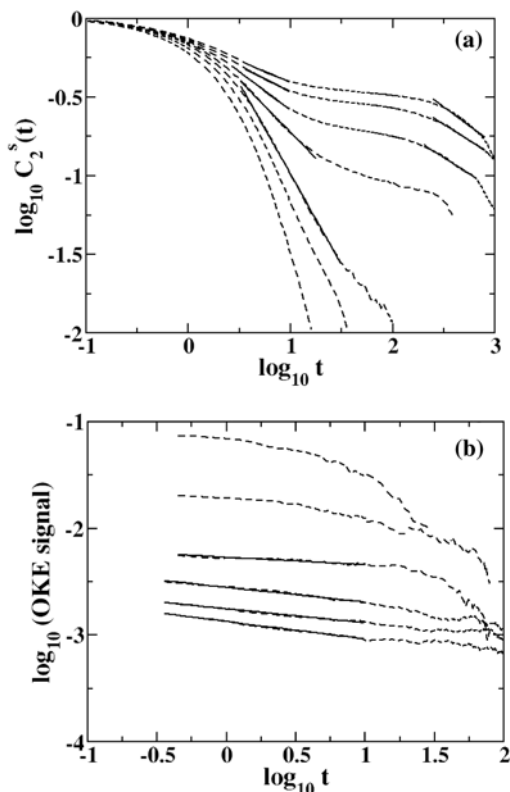
$$\varepsilon_1(\mathbf{e}_i, \mathbf{e}_j) = \left[1 - \chi^2 (\mathbf{e}_i \cdot \mathbf{e}_j)^2 \right]^{-1/2} \quad (5)$$

and

$$\varepsilon_2(\hat{\mathbf{r}}_{ij}, \mathbf{e}_i, \mathbf{e}_j) = 1 - \frac{\chi'}{2} \left[\frac{(\mathbf{e}_i \cdot \hat{\mathbf{r}}_{ij} + \mathbf{e}_j \cdot \hat{\mathbf{r}}_{ij})^2}{1 + \chi'(\mathbf{e}_i \cdot \mathbf{e}_j)} + \frac{(\mathbf{e}_i \cdot \hat{\mathbf{r}}_{ij} - \mathbf{e}_j \cdot \hat{\mathbf{r}}_{ij})^2}{1 - \chi'(\mathbf{e}_i \cdot \mathbf{e}_j)} \right] \quad (6)$$

with $\chi' = (\kappa'^{1/\mu} - 1)/(\kappa'^{1/\mu} + 1)$. Here $\kappa = \sigma_{ee}/\sigma_{ss}$ is the aspect ratio of the ellipsoid of revolution with σ_{ee} denoting the separation between two ellipsoids of revolution in a end-to-end configuration, and $\sigma_{ss} = \sigma_0$, and $\kappa' = \varepsilon_{ss}/\varepsilon_{ee}$, where ε_{ss} is the depth of the minimum of the potential for a pair of ellipsoids of revolution aligned in a side-by-side configuration, and ε_{ee} is the corresponding depth for the end-to-end alignment. Here ε_0 is the depth of the minimum of the pair potential between two ellipsoids of revolution aligned in cross configuration. The GB pair potential defines a family of models, each member of which is characterized by the values chosen for the set of four parameters κ , κ' , μ , and ν , and is represented by $GB(\kappa, \kappa', \mu, \nu)$ ¹¹. Systems consist of 500 ellipsoids of revolution in a cubic box with periodic boundary conditions at several temperatures, starting from the high-temperature isotropic phase down to the nematic phase across the I-N phase boundary have been simulated. We have carried out several simulations with different aspect ratios (κ) where for each aspect ratio isochors of different densities have been investigated. All quantities are given in reduced units defined in terms of the Gay-Berne potential parameters ε_0 and σ_0 : length in units of σ_0 , temperature in units of $\frac{\varepsilon_0}{k_B}$, and time in units of $\left(\frac{\sigma_0^2 m}{\varepsilon_0} \right)^{1/2}$, m being the mass of the ellipsoids of revolution. The mass as well as the moment of inertia of each of the ellipsoids of revolution have been set equal to unity. The intermolecular potential is truncated at a distance r_{cut} and shifted such that $U(r_{ij} = r_{cut}) = 0$, r_{ij} being the separation between two ellipsoids of revolution i and j . The equations of motion have been integrated using the velocity-verlet algorithm with integration time step $dt = 0.0015$.¹² Equilibration has been done by periodic rescaling of linear and angular velocities of particles. This has been done for a time period of t_q following which the system has been allowed to propagate with a constant energy for a time period of t_e in order to ensure equilibration upon observation of no drift of temperature, pressure, and potential energy. The data collection has been executed in a microcanonical ensemble. At each state point, local

Figure 1: The time evolution of the a) single particle OTCF on a log-log plot for GB(3,5,2,1) along an isochor with density $\rho=0.32$ across I-N transition at temperatures $T=2.008, 1.697, 1.499, 1.396, 1.310, 1.199$ and 1.102 from left to right and b) collective second rank OTCF for the same system and isochor at temperatures $T=2.008, 1.499, 1.396, 1.310, 1.199$ and 1.102 from top to bottom. T_{I-N} is located between $T=1.499$ and $T=1.396$. The portions fitted with straight line correspond to power law decay regime.



potential energy minimization has been executed by the conjugate gradient technique for a subset of 200 statistically independent configurations. The landscape analysis has been done with a system size of 256 ellipsoids of revolution, which is big enough for having no qualitative change in the results due to the system size.¹⁴ Minimization has been performed with three position coordinates and two Euler angles for each particle, the third Euler angle being redundant for ellipsoids of revolution.

B. Disk-like molecules

The parameterization, that we have employed here, is $\kappa = 0.345$, $\kappa' = 0.2$, $\mu = 1$, $\nu = 2^{11}$. Molecular dynamics simulations have been performed with the model discotic system containing 500 oblate ellipsoids of revolution in a cubic box with periodic boundary conditions. All the quantities reported here are given in reduced units. The intermolecular potential has been truncated at a distance $r_{\text{cut}} = 1.6$

and shifted. The equations of motion have been integrated following the velocity-Verlet algorithm with the integration time steps of $dt = 0.0015$ in the reduced units. Equilibration has been done in an NPT ensemble. Following this, the system has been allowed to propagate with a constant energy and density in order to ensure equilibration. Upon observation of no drift in temperature, pressure, and potential energy, the data collection has been executed in a microcanonical ensemble. The model discotic system has been melted from an initial fcc configuration at high temperatures and low densities, and studied along two isobars at pressures $P = 25$ and $P = 10$ at several temperatures.

Results and discussion

A. Calamitic liquid Crystals (rod-like molecules)

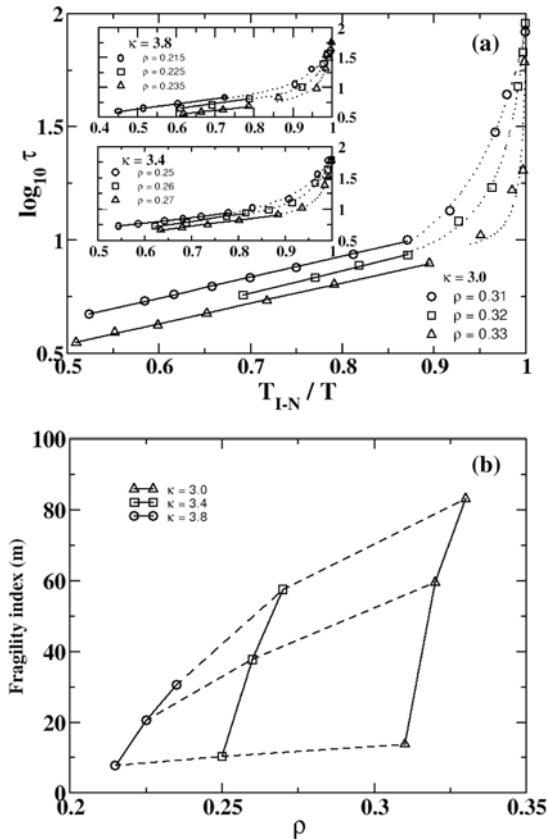
I. Single particle orientational dynamics

The orientational dynamics of the system at the single particle level may be described by the first and second order single particle orientational time correlation functions (OTCF) $C_l^s(t)$ ($l = 1, 2$), which are defined by

$$C_l^s(t) = \frac{\langle \sum_i P_l(e_i(t)) \cdot e_i(0) \rangle}{\langle \sum_i P_l(e_i(0)) \cdot e_i(0) \rangle} \quad (7)$$

where P_l is the l -th rank Legendre polynomial and the angular brackets stand for ensemble averaging. Figure 1a shows the single particle second rank OTCF in a log-log plot as the temperature is lowered from high temperature isotropic phase to low temperature nematic phase across the I-N transition. The I-N transition is marked by a jump in the orientational order parameter S , defined for an N -particle system as the largest eigenvalue of the ordering matrix Q : $Q_{\alpha\beta} = \frac{1}{N} \sum_{i=1}^N \frac{1}{2} (3e_{i\alpha}e_{i\beta} - \delta_{\alpha\beta})$, where $e_{i\alpha}$ is the α -component (in the space-fixed frame) of the unit orientation vector e_i along the principal symmetry axis of the i -th ellipsoid of revolution.¹⁵ Note the emergence of the power law decay at short to intermediate times near the I-N phase boundary. As the I-N phase boundary is crossed upon cooling, the advent of two power law decay regimes separated by an intervening plateau at short-to-intermediate times imparts a step-like feature to the temporal behavior of the second rank OTCF. Such power law relaxation near I-N phase boundary was an area of great interest in the recent past¹⁶⁻²¹ and it has been investigated that the scenario is not a unique property of the model we have studied; it is a rather universal phenomenon of second rank OTCF.¹² Such a feature bears remarkable similarity to what is observed for supercooled liquids as the glass transition is approached from the above.^{22,23} While for the supercooled liquid the emergence of step-like feature is well understood as a consequence of β relaxation, the origin of such a feature observed for liquid crystal defied of reliable explanation.

Figure 2: a) The orientational correlation time in the logarithmic scale as function of the inverse of the scaled temperature, the scaling being done by the isotropic to nematic transition temperature T_{I-N} . For the insets, the horizontal and the vertical axis labels read same as that of the main frame and are thus omitted for clarity. Along each isochor, the solid line is the Arrhenius fit to the subset of the high-temperature data and the dotted line corresponds to the fit to the data near the isotropic-nematic phase boundary with the VFT form. b) The fragility index m shown as a function of density for different aspect ratios. The dashed lines are guide to the eye to illustrate the fact that the dependence of the fragility index on the density is becoming stronger as the aspect ratio becomes smaller.



II. Collective orientational dynamics

In experiments, one can probe orientational relaxation through the decay of the OKE signal, which is given by the negative of the time derivative of the collective second rank OTCF $C_2^c(t)$.^{4,24,25} The latter is defined by

$$C_2^c(t) = \frac{\left\langle \sum_i \sum_j P_2(e_i(0) \cdot e_j(t)) \right\rangle}{\left\langle \sum_i \sum_j P_2(e_i(0) \cdot e_j(0)) \right\rangle}. \quad (8)$$

Calculation of this correlation function is computationally demanding, particularly at longer times. In order to set a direct link with experimental results, we show the temporal behavior of the OKE signal in the log-log plot for the system across the

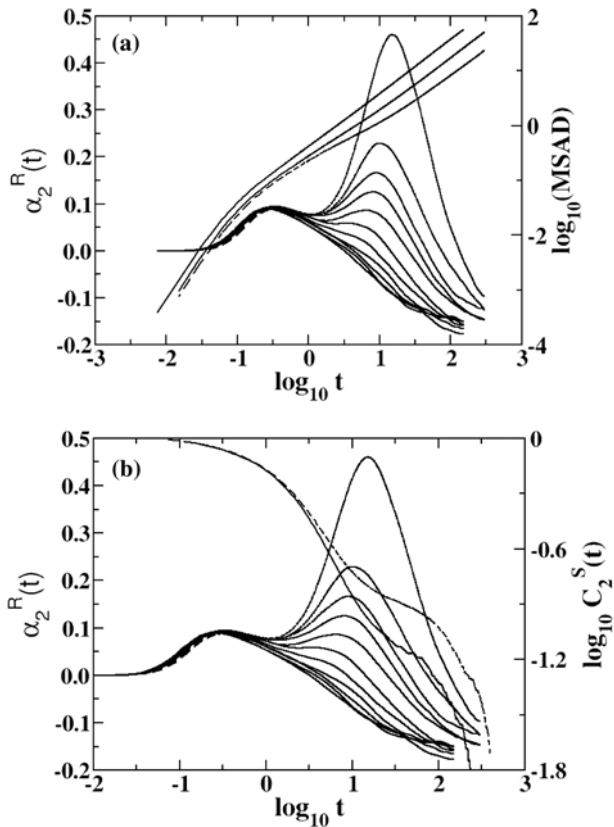
I-N phase transition in figure 1b. The short-to-intermediate-time power law regime is evident in the OKE signal for the system studied here. Like single particle second rank OTCF, it is also verified to be a universal phenomenon near I-N transition.¹²

III. Fragility of liquid crystals

We estimate the orientational correlation time τ as the time taken for $C_2^c(t)$ to decay by 90%, i.e., $C_2^c(t = \tau) = 0.1$. Figure 2(a) shows τ in the logarithmic scale as a function of the inverse temperature along the three isochors for each of the three systems considered. We have scaled the temperature by T_{I-N} in the spirit of Angell's plot, that displays the shear viscosity (or the structural relaxation time, the inverse diffusivity, etc.) of glass-forming liquids as a function of the inverse of the scaled temperature, the scaling being done in the latter case by the glass transition temperature T_g .^{26,27} For all the three systems, two distinct features are common: (i) in the isotropic phase far away from the I-N transition, the orientational correlation time τ exhibits the Arrhenius temperature dependence, i.e., $\tau(T) = \tau_0 \exp(E/k_B T)$, where the activation energy E and the pre-factor τ_0 are both independent of temperature; (ii) in the isotropic phase near the I-N transition, the temperature dependence of τ shows marked deviation from the Arrhenius behavior and can be well described by the Vogel-Fulcher-Tammann (VFT) equation $\tau(T) = \tau_0 \exp[B/(T - T_{VFT})]$, where τ_0 , B , and T_{VFT} are constants, independent of temperature. Again these features bear remarkable similarity with those observed for fragile glass-forming liquid. A non-Arrhenius temperature behavior is taken to be the signature of fragile liquids. For fragile liquids, the temperature dependence of the shear viscosity follows the Arrhenius behavior far above T_g and can be fitted to the VFT functional form in the deeply supercooled regime near T_g .^{26,27} The striking resemblance in the dynamical behavior described above between the isotropic phase of thermotropic liquid crystals near the I-N transition and supercooled liquids near the glass transition has prompted us to attempt a quantitative measure of glassy behavior near the I-N transition. For supercooled liquids, one quantifies the dynamics by a parameter called fragility index which measures the rapidity at which the liquid's properties (such as viscosity) change as the glassy state is approached. In the same spirit²⁸ that offers a quantitative estimation of the fragile behavior of supercooled liquids, we here define the fragility index m of a thermotropic liquid crystalline system as²¹

$$m = \left. \frac{d \log_{10} \tau(T)}{dT_{I-N}/T} \right|_{T=T_{I-N}}. \quad (9)$$

Figure 3: Time evolution of the rotational non-Gaussian parameter $\alpha_2^R(t)$ in a semi-log plot for the system with aspect ratio $\kappa=3$. The time dependence is shown at several temperatures ($T=3.5, 3.25, 3.0, 2.75, 2.5, 2.25, 2.0, 1.88, 1.82, 1.78$, and 1.5) across the isotropic-nematic (I-N) transition along an isochor at density $= 0.33$. a) On a different scale along the vertical axis (appearing on the right), time evolution of the mean square angular deviation ($\Delta\phi^2(t)$) is shown in a log-log plot for three temperatures: the highest temperature studied in the isotropic phase ($T=1.5$) and the other two temperatures ($T=3.0$ and 2.75) that are closest to the I-N transition on either side along with the time evolution of $\alpha_2^R(t)$, and b) On a different scale along the vertical axis (appearing on the right), the time evolution of the single-particle second rank orientational time correlation function $C_2^s(t)$ is shown in a log-log plot for the two temperatures ($T=3.0$ and 2.75) that are closest to the I-N transition on either side along with the time evolution of $\alpha_2^R(t)$. The solid lines denote the curves for the high temperature isotropic phase and the dashed lines for the low temperature nematic phase.



It is clear from the above equation that if $\tau(T)$ follows Arrhenius temperature dependence, m will be constant throughout the whole temperature range. Figure 2(b) shows the density dependence of the fragility index for the three systems with different aspect ratios. For a given aspect ratio, the fragility index increases with increasing density, the numerical values of the fragility index m being comparable to those of supercooled liquids. The density dependence observed in the present work is remarkably similar to those observed for supercooled liquids. For the range of aspect ratios

studied here, the dependence of the fragility index on the density is becoming stronger as the aspect ratio becomes smaller.

IV. Heterogeneous dynamics

Another hallmark of fragile glass-forming liquids is spatially heterogeneous dynamics²⁹ reflected in non-Gaussian dynamical behavior.³⁰ It is intuitive that the growth of the pseudo-nematic domains, characterized by local nematic order, in the isotropic phase near the I-N transition would result in heterogeneous dynamics in liquid crystals. We have, therefore, monitored the time evolution of the rotational non-Gaussian parameter (NGP),^{31,32} $\alpha_2^R(t)$, which in the present case is defined as

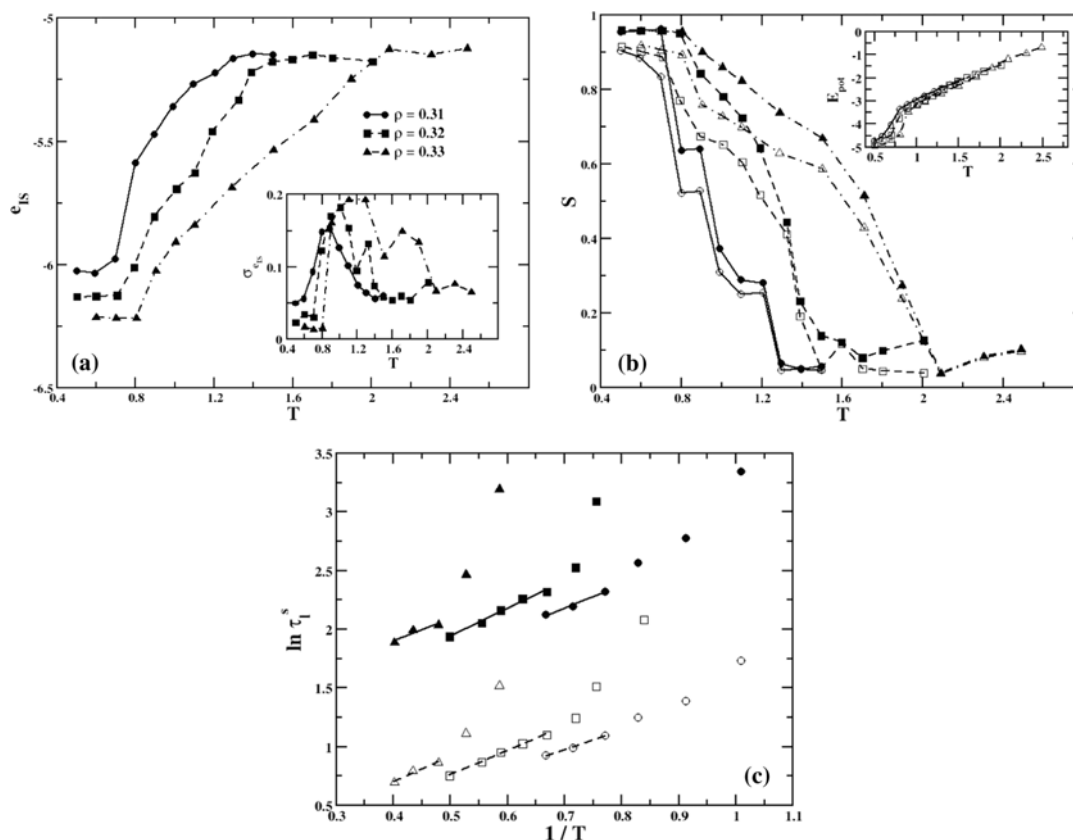
$$\alpha_2^R(t) = \frac{\langle \Delta\phi^4(t) \rangle}{2\langle \Delta\phi^2(t) \rangle^2} - 1 \quad (10)$$

where

$$\langle \Delta\phi^{2n}(t) \rangle = \frac{1}{N} \sum_{i=1}^N \langle |\phi_i(t) - \phi_i(0)|^{2n} \rangle. \quad (11)$$

Here ϕ_i is the rotation vector like the position vector r_i appears in the case of translational NGP of i th ellipsoid of revolution, the change of which is defined by $\Delta\phi_i(t) = \phi_i(t) - \phi_i(0) = \int_0^t dt' \omega(t')$, ω_i being the corresponding angular velocity,^{22,23} and N is the number of ellipsoids of revolution in the system. NGP will have value equal to zero when system dynamics is spatially homogeneous and will have a non-zero value when the system dynamics is spatially heterogeneous. As a typical behavior, Fig. 3(a) and (b) show the time dependence of the rotational NGP for one of the systems at several temperatures across the I-N transition along an isochor. On approaching the I-N transition upon cooling, a bimodal feature starts appearing with the growth of a second peak, which eventually becomes the dominant one, at longer times.^{21,31} We further investigate the appearance of this bimodal feature in NGP plot. To this end we calculate mean square angular deviation (MSAD) of the system at different temperatures starting from high temperature isotropic phase to low temperature nematic phase. The appearance of the bimodal feature in the rotational NGP is accompanied by a signature of a sub-diffusive regime in the temporal evolution of the MSAD, the time scale of the short-time peak and that of the onset of the sub-diffusive regime being comparable, as shown in Fig. 3(a).^{21,31} We note that the dominant peak appears on a time scale which is comparable to that of onset of the diffusive motion in orientational degrees of freedom

Figure 4: a) The temperature dependence of the average inherent structure energy per particle e_{IS} along three isochors at densities $\rho=0.31, 0.32$, and 0.33 for $\kappa=3$. The inset shows the root mean square fluctuation in inherent structure energy $\sigma_{e_{IS}}$, computed from a subset of 200 configurations for each state point, as a function of temperature T at the same three densities. b) The evolution of the average order parameter S with temperature both for the inherent structures (filled) and the corresponding pre-quenched ones (empty). The inset shows the temperature dependence of the average potential energy E_{pot} at a state point obtained from averaging over the molecular dynamics trajectory. For clarity, E_{pot} is shown for the state points along only one isochor corresponding to the density $\rho=0.32$. The state points considered in our simulations correspond to (i) the isotropic (I) phase for $T \geq 1.297$ and the smectic-B (Sm-B) phase for $T \leq 0.595$ along the isochor at $\rho=0.31$; (ii) I for $T \geq 1.495$ and Sm-B for $T \leq 0.706$ at $\rho=0.32$; (iii) I for $T \geq 2.089$ and Sm-B for $T \leq 0.803$ at $\rho=0.33$. c) The inverse temperature dependence of the single-particle orientational relaxation times τ_l^i , $l=1$ (filled) and $l=2$ (empty), in the logarithmic scale. The straight lines are the Arrhenius fits for the subsets of data points, each set corresponding to a fixed density: $\rho=0.31$ (circle), $\rho=0.32$ (square), $\rho=0.33$ (triangle up).



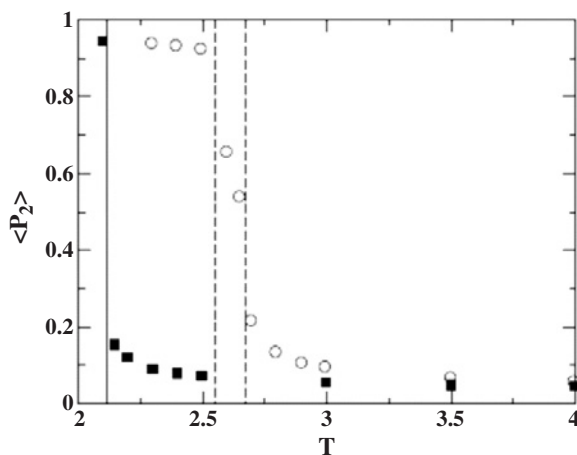
(ODOF) as evident in Fig. 3(a).^{21,31} Similar feature has been observed recently for supercooled water.³¹ We further find that the time scale at which the long-time peak appears is also comparable to the time scale of onset of the plateau that is observed in the time evolution of $C_2^S(t)$, as shown in Fig. 3(b).^{21,31}

V. Energy landscape analysis

Several studies have attempted to interpret the dynamics of glass-forming liquids in terms of the features of the underlying energy landscapes.^{33–38} Energy landscape analysis gives the potential energy, which devoid of any kind of thermal motions, of inherent structures of the parent liquid and hence provides a better understanding of the structure and

dynamics of the parent liquid. Figure 4a displays the average inherent structure energy as the change in temperature drives the system across the mesophases along three different isochors. Figure 4b shows the concomitant evolution of the average orientational order parameter S both for the inherent structures and the corresponding pre-quenched ones. It is evident that the average inherent structure energy remains fairly insensitive to temperature in the isotropic phase before it starts undergoing a steady fall below a certain temperature that corresponds to the onset of the growth of the orientational order¹⁴. As the orientational order grows through the nematic phase, the system continues to explore deeper potential energy minima until a plateau is reached on arrival at the smectic phase¹⁴. In the

Figure 5: The average second-rank orientational order parameter $\langle P_2 \rangle$ as a function of temperature along two isobars. The circles correspond to the data for the pressure $P=25$ and the squares for $P=10$. The phase boundaries are shown by vertical dotted lines for $P=25$ and by a vertical solid line for $P=10$.



inset of Fig. 4a, the location of the maximum of the mean square fluctuation in the inherent structure energy shows that the system explores potential energy minima spanning over a broader energy range as it settles into the nematic phase. This suggests the critical role of fluctuation effects in the nematic phase. The average potential energy for a state point obtained from the molecular dynamics trajectory, however, decreases rather smoothly in all three phases with decrease in temperature as illustrated in the inset of Fig. 4b. It is evident that the signature of the I–N transition is quite weak here in contrast to that of the nematic–smectic transition. We have repeated the same analysis for a larger system size to check the effect of finite system size, but qualitatively ended up with same conclusions as the smaller one. Note that this has been observed for a glassy system,³⁶ where the average IS energy also falls over a temperature range.³⁴ Like supercooled liquid, we have also observed a Gaussian form of number density of IS with e_{IS} .²¹

Figure 4c illustrates the correlation of the energy landscape behaviour with the dynamics the system exhibits. Here, we define relaxation times $\tau_l^s(T)$ as the time when $C_l^s(t) = e^{-1}$.¹⁴ The dramatic slow down of orientational dynamics with decreasing temperature near the I–N transition manifests in the temperature dependence of these relaxation times. Figure 4c shows that in the isotropic phase far from the I–N transition region $\tau_l^s(T)$ exhibits the Arrhenius behavior, i.e., $\tau_l^s(T) = \tau_{0,l} \exp[E_l/(k_B T)]$, where the activation energy E_l and the infinite temperature relaxation time $\tau_{0,l}$ are independent of temperature. We find

that the breakdown of the Arrhenius behavior occurs at a temperature that marks the onset of the growth of the depth of the potential energy minima explored by the system.¹⁴ Such correlations of different other properties with the landscape have been investigated in several other studies for both supercooled liquids and thermotropic liquid crystals.^{39,40}

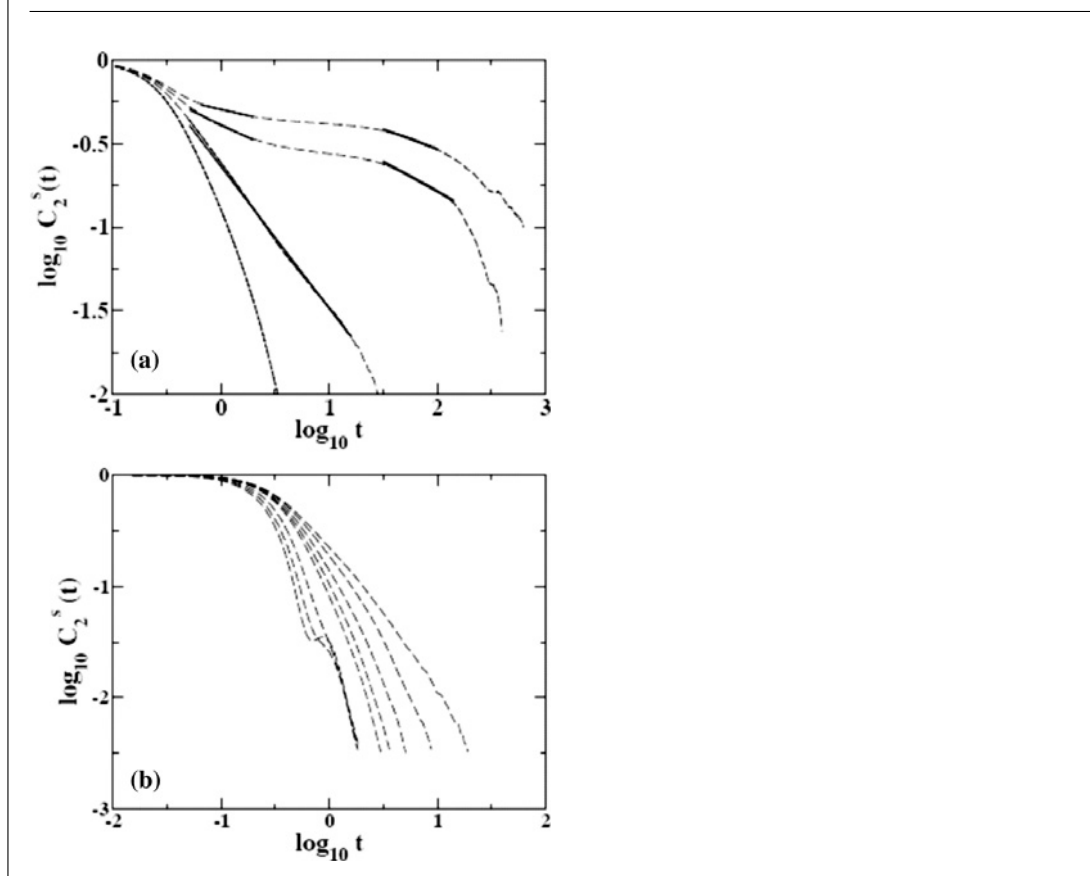
B. Discotic liquid crystals (disk-like molecules)

We first need to characterize the phases that appear along the isobars studied here. To this end, we have monitored the average second-rank orientational order parameter $\langle P_2 \rangle$. $\langle P_2 \rangle$ tends to zero in the isotropic phase but retains a non-zero value because of the finite size of the system. In the nematic phase, $\langle P_2 \rangle$ has a value above 0.4. For the columnar phase, $\langle P_2 \rangle$ is above 0.9. In the present case, we observe the I–N–C phase sequence along the isobar at the higher pressure and the sequence I–C along the other isobar. The temperature dependence of $\langle P_2 \rangle$ has been shown in Figure 5.

I. Single particle orientational dynamics

We have investigated orientational dynamics at the single-particle level by monitoring the temporal evolution of the corresponding second-rank orientational time correlation functions (OTCF). In Fig. 6, we show the time evolution of the single-particle second-rank OTCF at several temperatures in log-log plots. The emergence of a power law decay at short-to-intermediate times near the I–N phase boundary is notable in Fig. 6(a). It follows from Fig. 6(a) that as the system transits

Figure 6: Time evolution of the single-particle second-rank OTCF in log-log plots for the discotic system at several temperatures. The dashed lines are the simulation data corresponding to increasing orientational order parameter from the bottom to the top. The solid lines are the linear fits to the data, showing the power law decay regimes. (a) Along the isobar at $P=25.0$ at several temperatures: $T=2.991, 2.693, 2.646,$ and 2.594 ; (b) Along the isobar at $P=10.0$ at all the temperatures studied for the isotropic phase.



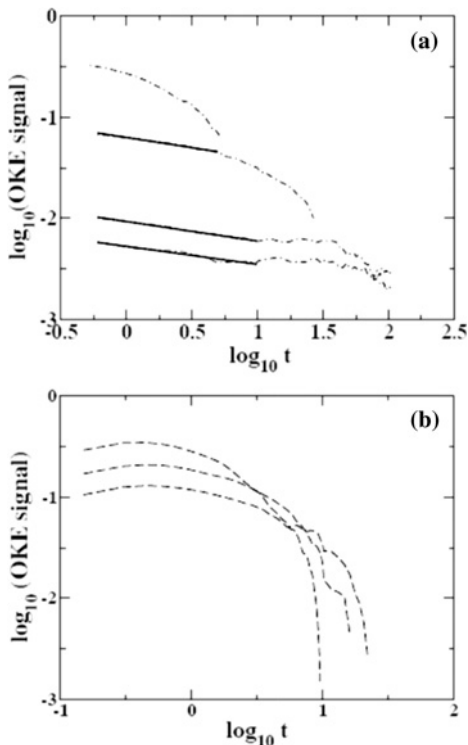
across the I–N phase boundary, two power law relaxation regimes, separated by a plateau, appear giving rise to a step-like feature. However, the decay of the single-particle second-rank OTCF in the isotropic phase near the isotropic-columnar phase boundary does not follow any power law as evident in 6(b).

II. Collective orientational dynamics

In optical heterodyne detected optical Kerr effect measurements (OHD-OKE), one probes collective orientational relaxation⁴¹. In recent OHD-OKE experiments with calamitic liquid crystals, the decay of the OKE signal has been found to follow a complex pattern.^{3,4} The most intriguing feature has been the power law decay regimes at short-to-intermediate times.^{4,5} We have therefore monitored the time evolution of the collective second-rank OTCF. In the present case, the negative of the time derivative of the collective second-rank OTCF provides a measure of the experimentally observable

OHD-OKE signal. As monitoring the time evolution of collective orientational correlation function is computationally quite demanding, we have restricted ourselves to the short-to-intermediate time dynamics that would suffice to compare the most intriguing aspect of the experimental observations. In Fig. 7, we show in log-log plots the temporal behavior of the OKE signal derived from present system at several temperatures. A short-to-intermediate-time power law regime is evident in the decay of the OKE signal on either side of the I–N transition as illustrated in Fig. 7(a). In consistency with the single-particle dynamics, such a power law decay regime is not observed for the OKE signal in the isotropic phase near the I–C phase boundary as apparent in Fig. 7(b). It follows from the time evolution of the single-particle second-rank OTCF shown in Fig. 6(a) that as the system settles into the nematic phase, two power law decay regimes, that are separated by a plateau, emerge. Such a feature bears a close resemblance with what has been

Figure 7: The short-to-intermediate time decay of the OKE signal in log-log plots for the discotic system. The dashed lines are the simulation data and the solid lines show the linear fits to the data showing the power law decay regimes: $\sim t^{-\alpha}$. The values of the power law exponent α are given below in the parenthesis. (a) Along the isobar at $P=25.0$ at several temperatures: $T=2.991$, $T=2.693$ ($\alpha=0.208$), $T=2.646$ ($\alpha=0.194$), and $T=2.594$ ($\alpha=0.178$). (b) Along the isobar at $P=10.0$ at several temperatures: $T=2.298$, 2.196 , and 2.143 . Temperature decreases from the top to the bottom at the left of the figure in each case.



observed recently for a model system of calamitic liquid crystals²¹. The decay pattern is also similar to those observed for models supercooled molecular liquids. In fact, based on a series of OHD-OKE measurements Fayers and coworkers have recently drawn an analogy in the orientational dynamics between calamitic liquid crystals in their isotropic phase near the I–N transition and supercooled molecular liquids. The analogous dynamics could be captured in a subsequent molecular dynamics simulation study of model systems of these two classes of soft condensed matter. The short-to-intermediate time power law decay of the OKE signal observed therein bears a close similarity with what is found in the present discotic system across the I–N transition. The contrasting behavior observed in orientational relaxation in the isotropic phase near the I–N and the I–C phase boundaries is noteworthy. Such an observation may throw new light on the origin of the power law relaxation in the isotropic phase near the I–N transition.

While the I–C transition is strongly first order in nature, the I–N transition is only weakly first order with certain characteristics of the continuous transition. This is reflected in the present case in a much larger change in the density marking the I–C transition as compared to the I–N transition (data not shown). The weakly first order nature of the I–N transition appears to play a role in the short-to-intermediate time power law relaxation. It seems fair to trace the origin of the power law decay in orientational relaxation to the growth in the orientational correlation length in the isotropic phase near the I–N transition.

III. Theoretical analysis

The I–N phase transition is weakly first order both in calamitic and discotic systems. This is manifested in the growing orientational pair correlation length as the I–N phase boundary is approached from the high temperature isotropic phase. Apparently, a second order phase transition at a temperature only slightly lower (by ≈ 1 K), where the orientational correlation length would have diverged, is preempted by the weakly first order phase transition. Nevertheless, even this weakly first order phase transition is driven by the growing correlation length. The temperature dependent growth of this correlation length $\xi(T)$ can be given by the following expression¹

$$\xi(T) = A(T^* - T)^{-\nu} \quad (12)$$

where ν is 0.5 in the Landau mean-field theory. A simple mode coupling theory, based on time dependent density functional theory, shows that this growing correlation length can give rise to a power-law decay of the type observed in simulations. This approach uses the the generalized Debye–Stokes–Einstein relation between the correlation time, diffusion, and friction⁴²

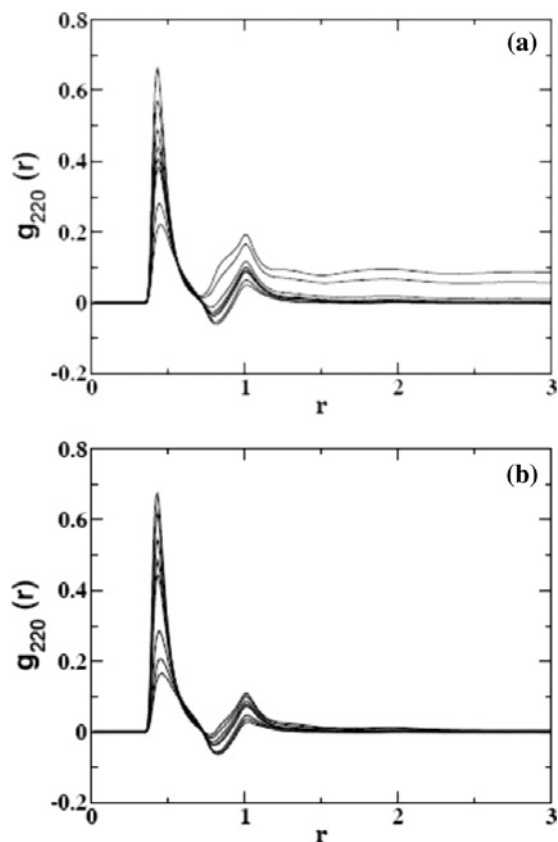
$$C_2(z) = \frac{1}{(z + 6AD_R(z))} \quad (13)$$

and

$$D_R(z) = \frac{k_B T}{I(z + \zeta(z))} \quad (14)$$

where A is equal to 1 for the single-particle relaxation, but is related to orientational caging for collective dynamics. It was shown elsewhere, the growing correlation length can give rise to a singular frequency dependence of ζ over a frequency range $\zeta(z) \sim A/z^\alpha$ with $\alpha = 0.5$. This power law dependence in the frequency dependence of friction in turn gives rise to a power law decay in the orientational time correlation function.

Figure 8: The orientational pair distribution function $g_{220}(r)$ for the model discotic system at state points along two isobars: (a) the one at $P=25$ and (b) the other at $P=10$. The temperature decreases from the bottom to the top at the position of the dominant peak of the curves starting from high temperature isotropic phase down to the temperature which is just above the temperature at which columnar phase appears.



IV. Orientational pair correlation function

Thus, in the above mentioned theory, the origin of the power law decay is essentially the same as observed near the critical phenomena. However, one may not expect a universal behavior since there is no true divergence. The absence of power law decay near the I–C phase boundary could then be due to the absence of any growing correlation length. The I–C phase transition is strongly first order in nature where both orientational and positional order set in at the same time. Since the growth of orientational correlation is small, a power law decay is not expected. To verify our assertion, we have calculated the distance dependent orientational pair distribution function $g_{l'm}(r)$ ⁴³ for the system studied here along both the isobars and presented in Fig. 8(a) and Fig. 8(b), respectively. While the growth of orientational correlation length is clearly evident across the I–N transition, such a growth is found to be totally absent in the isotropic phase near the I–C phase boundary.

Conclusion

We have presented theoretical and computer simulation studies of dynamics of calamitic and discotic liquid crystals, both near the I–N phase boundary and also in the respective liquid crystalline phases. Computer simulation studies of single particle and collective orientational dynamics of thermotropic liquid crystals near the isotropic–nematic (I–N) transition are presented and compared with the dynamics of supercooled liquids near glass transition. The short-to-intermediate time scale power law decay in the orientational relaxation appeared to be the most intriguing feature. In analogy with the supercooled liquids, a fragility index of liquid crystals is introduced to quantify the glassiness of orientational dynamics near the I–N transition. Our investigation of spatially heterogeneous dynamics strengthens the analogy further. The striking resemblance in the correspondence between the manner of the exploration of the potential energy landscape and the onset of the non-Arrhenius temperature dependence of the relaxation time might imply a unique underlying landscape mechanism for slow dynamics in soft condensed matter.

In the second part of study, of disk-like molecules, the system has been studied along two isobars so chosen that the phase sequence I–N–C appears upon cooling along the one and the sequence I–C along the other. We have investigated temperature dependent orientational relaxation across the I–N transition and in the isotropic phase near the I–C phase boundary with a focus on the short-to-intermediate time decay behavior. While the orientational relaxation across the I–N phase boundary again shows a power law decay at short-to-intermediate times, such power law relaxation is not observed in the isotropic phase near the I–C phase boundary. Study of orientational pair distribution function shows that there is a growth of orientational pair correlation near the I–N transition whereas such a growth is absent in the isotropic phase near the I–C phase boundary. As the system settles into the nematic phase, the decay of the single-particle second-rank orientational time correlation function follows a pattern that is similar to what is observed with calamitic liquid crystals and supercooled molecular liquids.

The present study brings out the role of intermolecular correlations in giving rise to the power law, in a way quite similar to the emergence of such effects in supercooled liquids, except that here the fluctuations due to a weakly first order phase transition makes the effects much more pronounced, as evident from experiments and simulations. Energy landscape analysis provides a convincing testimony to this observation.

Future work may look into the relaxation dynamics of discotic liquid crystals more extensively. As already mentioned, this system has not been studied in adequate detail. Another greatly interesting system is calamitic liquid crystals of dipolar rod-like molecules because many real molecular systems are dipolar. Such a system can exhibit dynamics distinctive of the system. Only a few studies exist along this line⁴⁴.

Acknowledgement

It is a great pleasure to thank Dr. Dwaipayana Chakrabarti for helpful suggestions and discussions during the preparation of the manuscript. This work was supported in part by a grant from DST, India. BJ thanks CSIR, India for providing SRF.

Received 15 April 2009.

References

- de Gennes P G and Prost J 1993 *The Physics of Liquid Crystals* (Clarendon Press, Oxford).
- Chandrasekhar S 1992 *Liquid Crystals* (Cambridge University Press, Cambridge).
- Gottke S D, Bruce D D, Cang H, Bagchi B and Fayer M D 2002 *J. Chem. Phys.* **116** 360.
- Gottke S D, Cang H, Bagchi B and Fayer M D 2002 *J. Chem. Phys.* **116** 6339.
- Cang H, Li J, Novikov V N and Fayer M D 2003 *J. Chem. Phys.* **118** 9303.
- Chandrasekhar S, Sadashiva B K and Suresh K A 1977 *Pramana* **9** 471.
- Chandrasekhar S and Ranganath G S 1990 *Rep. Prog. Phys.* **53** 57.
- Hindmarsh P, Hird M, Styring P and Goodby J W 1993 *J. Mater. Chem.* **3** 1117.
- Allen M P, Evans G T, Frenkel D and Mulder B M 1993 *Adv. Chem. Phys.* **86**, 1.
- Gay J G and Berne B J 1981 *J. Chem. Phys.* **74** 3316.
- Bates M A and Luckhurst G R 1999 *J. Chem. Phys.* **110** 7087.
- Chakrabarti D, Jose P P, Chakrabarty S and Bagchi B 2005 *Phys. Rev. Lett.* **95** 197801.
- Ilnytskyi J M and Wilson M R 2002 *Comput. Phys. Commun.* **148** 43.
- Chakrabarti D and Bagchi B 2006 *Proc. Natl. Acad. Sci. USA* **103** 7217.
- Zannoni C 2000 in *Advances in the Computer Simulations of Liquid Crystals*, eds. Pasini P and Zannoni C (Kluwer Academic Publishers, Dordrecht) pp. 17–50.
- Jose P P and Bagchi B 2004 *J. Chem. Phys.* **120** 11256.
- Jose P P and Bagchi B 2006 *J. Chem. Phys.* **125** 184901.
- Chakrabarty S, Chakrabarti D and Bagchi B 2006 *Phys. Rev. E* **73** 061706.
- Chakrabarti D, Jana B and Bagchi B 2007 *Phys. Rev. E* **75** 061703.
- Chakrabarti D and Bagchi B 2007 *J. Phys. Chem. B* **111** 11646; 2007 *J. Chem. Phys.* **126** 204906; 2009 *Adv Chem Phys* **141** (in press).
- Jana B, Chakrabarti D and Bagchi B 2007 *Phys. Rev. E* **76** 011712.
- Kämmerer S, Kob W and Schilling R 1997 *Phys. Rev. E* **56** 5450.
- Michele C De and Leporini D 2001 *Phys. Rev. E* **63** 036702.
- (a) Yan Y -X and Nelson K A 1987 *J. Chem. Phys.* **87** 6240; (b) Yan Y -X and Nelson K A 1987 *J. Chem. Phys.* **87** 6257.
- Li J, Wang I and Fayer M D 2005 *J. Phys. Chem. B* **109** 6514.
- Angell C A 1988 *J. Phys. Chem. Solids* **49** 863.
- Angell C A 1991 *J. Non-Cryst. Solids* **131-133** 13.
- Böhmer R, Ngai K L, Angell, C A and Plazek D J 1993 *J. Chem. Phys.* **99** 4201.
- Ediger M D 2000 *Ann. Rev. Phys. Chem.* **51** 99.
- Shell M S, Debenedetti P G and Stillinger F H 2005 *J. Phys.: Condens. Matter* **17** S4035.
- Jose P P, Chakrabarti D and Bagchi B 2006 *Phys. Rev. E* **71** 030701(R).
- Mazza M G, Giovambattista N, Starr F W and Stanley H E 2006 *Phys. Rev. Lett.* **96** 057803.
- Wales D J 2003 *Energy Landscapes* (Cambridge University Press, Cambridge).
- Sastry S, Debenedetti P G and Stillinger F H 1998 *Nature* **393** 554.
- Scala A, Starr FW, Nave E L, Sciortino F and Stanley H E 2000 *Nature* **406** 166.
- Sastry S 2001 *Nature* **409** 164.
- Martinez L -M and Angell C A 2001 *Nature* **410** 633.
- Salka-Voivod I, Poole P H and Sciortino F 2001 *Nature* **412** 514.
- Chakrabarti D and Bagchi B 2006 *Phys. Rev. Lett.* **96** 187801.
- Chakrabarti D and Bagchi B 2006 *Phys. Rev. E* **74** 041704.
- Torre R, Bartolini P and Pick R M 1998 *Phys. Rev. E* **57** 1912.
- Bagchi B and Bhattacharyya S 2003 *Adv. Chem. Phys.* **116** 67.
- Allen M P and Tildesley D J *Computer simulation of liquids* (Clarendon Press, Oxford, 1987).
- Zhou H -X and Bagchi B 1992 *J. Chem. Phys.* **97** 3610.



and biomolecular hydration.

Biman Jana did his undergraduate study from Calcutta University, West Bengal and master study from Indian Institute of Technology, Kanpur. He is currently pursuing his doctoral degree at Indian Institute of Science, Bangalore under the supervision of Prof. Biman Bagchi. His research focuses on understanding the dynamics of complex systems which includes liquid crystals



Biman Bagchi obtained his Ph.D. degree from Brown University in 1981 with Professor Julian H. Gibbs. He was Research Associate at University of Chicago (1981–1983), where he worked with Professors David W. Oxtoby, Graham Fleming, and Stuart Rice, and at University of Maryland (with Robert Zwanzig) before returning to India in 1984 to join as faculty in Indian Institute of Science, Bangalore. He is a Fellow of the Indian Academy of Sciences, Indian National Academy of Science and also of the Third World Academy, Trieste. His research interests include statistical mechanics, relaxation phenomenon, chemical reaction dynamics, phase transitions, protein folding and enzyme kinetics.